Comparison of Responses Between Human Body Model and Anthropomorphic Test Device Model in Reclined Postures

Jing Fei, Yu Liu, Peifeng Wang, XiaoTing Yang, Zhen Li, Lingwei Zhang,
Qiang Wang, Xinming Wan

Abstract The advanced autonomous driving system enables more flexible seating arrangements. While a reclined seat can enhance comfort during the ride, it may also significantly affect kinematic response of the occupants. Currently, there are two common virtual tools for studying occupant injury: Human Body Models and Anthropomorphic Test Device Models. The differences in the internal structural responses of these two groups under reclined postures are not well understood. This study focuses on analyzing the kinematic and mechanical response of occupants' pelvis and lumbar spine under rigid seat with zero gravity characteristics. Four seat conditions were designed, altering angle of seat-back, seat pan, and leg rest. Simulations were conducted using THUMS v6.1 and THOR-AV model for highly reclined angle research, subjecting them to a 47 km/h frontal crash pulse on a sled. The study found that as the recline angle increases, the forward movement of the pelvis increased, which led to increased interaction forces between the pelvis and lap belt, and increased compression forces on the lumbar spine. In addition, raising the seat pan could help reduce the forces on the pelvis and lumbar spine. THOR-AV and THUMS align well in pelvic forward motion but show clear differences in pelvic rotation. There were also some differences in the degree of Z-direction movement of the head and torso. In particular, THUMS exhibits lumbar extension moments at high reclined angles, necessitating further research on the load-bearing and injury mechanisms of the occupants' lumbar spine in high reclined postures.

Keywords Reclined, Lumbar spine, pelvis, THOR-AV, THUMS.

I. INTRODUCTION

In vehicles equipped with advanced autonomous driving systems, the attention of drivers and occupants is freed from maneuvering the vehicle and observing the surrounding environment, leading to an expectation for a more comfortable ride experience. Novel reclined seats, particularly zero-gravity seats, can help occupants relax in future autonomous vehicles [1-3]. However, despite the implementation of advanced autonomous driving systems, traffic accidents remain inevitable [4, 5]. Preliminary studies suggest that existing passive safety systems may fail when occupants change their posture [6]. It is necessary to investigate the kinematic response and potential injuries of occupants in reclined postures during vehicle collisions to determine the effectiveness of current restraint systems and future countermeasures to better protect occupants.

Previous studies have focused on the motion and injury of the pelvis and lumbar spine in reclined seats, primarily using Post Mortem Human Subjects (PMHS) in sled impact tests to obtain dynamic responses of the human body in reclined postures. The University of Michigan Transportation Research Institute (UMTRI) conducted frontal sled tests on three mid-sized male PMHS using semi-rigid seats, revealing that a 45° seat inclination increased the likelihood of lumbar sacral and iliac wing fractures [7]. Richardson, R. et al. conducted frontal sled tests at 50 km/h on five male PMHS with a seat inclination angle of 50°, showing that the reclined posture reduced the effective restraint of the seat and seatbelt and increased the risk of submarining due to the initial posterior rotation of the pelvis [8-9]. Shin, J. et al.'s research also indicated lumbar fractures in both male and female PMHS in reclined postures [10].

Human Body Models (HBMs) are widely used in occupant safety research for vehicle crash simulations and are considered effective tools for studying injury patterns in reclined postures. Gepner, B. et al. conducted simulations using three different HBMs, including GHBMC v.6.0, THUMS v.6.0, and SAFER v.10, under reclined semi-rigid seat conditions based on PMHS test boundary conditions. The results showed that the seatbelt forces and trajectories of key areas in all HBMs were consistent with PMHS test data [11]. HBMs have been used in studies of restraint system parameters and occupant submarining and lumbar injuries in reclined seats [12-14].

X. Wan (e-mail: wanxm_2006@163.com; tel: +86 178 4376 1276) is a Research Scientist. Y. Liu, J. Fei, P. Wang and L. Zhang are Researchers at China Automotive Engineering Research Institute Co., Ltd., Chongqing, China. X. Yang and Z. Li are MS Students in Mechanical Engineering and Q. Wang is a PhD student in Mechanical Engineering at the State Key Laboratory of Advanced Design and Manufacturing Technology for Vehicle, Hunan University, Changsha, China.

On the other hand, for Anthropomorphic Test Devices (ATDs) widely used in current automotive safety crash tests, Shin, J. et al. demonstrated that due to limitations in hip and spine design, neither HIII-50M nor THOR-50M could adequately match the kinematic responses of PMHS in reclined postures, making them unsuitable for crash safety studies of zero-gravity seats [15]. The THOR-AV 50M is an improved dummy developed by Humanetics based on the THOR-50M [16]. Wang, J. et al. conducted comparative studies of the kinematic responses of the physical THOR AV 50M in reclined postures and PMHS tests, achieving higher BioRank scores [17]. However, this study lacked detailed analysis of lumbar and pelvic motion and injuries, and the existing PMHS and physical ATD test results do not allow direct observation and comparison of pelvis and lumbar spine motion patterns and loading mechanisms between humans and dummies.Both HBMs and advanced ATD Finite Element (FE) models can be used for simulating intrinsic structural responses and injuries in highly reclined postures. However, it remains unclear what differences exist in the pelvis and lumbar spine responses between these two models in reclined postures.

Therefore, this study focuses on the THUMS v.6.0 and THOR-AV 50M FE models as the research subjects, utilizing a typical Mobile Progressive Deformable Barrie (MPDB) pulse obtained from vehicle test statistics as input. It configures a rigid seat with zero gravity characteristics and an integrated three-point seatbelts, and sets up four different reclined seat postures. It thoroughly compares the kinematic and mechanical responses of key areas in various reclined postures between the two models. The results of this study can help understand the potential correlation between HBM and ATD crash injuries in highly reclined postures and serve as an initial attempt to establish a mapping relationship between HBM and ATD injuries. Furthermore, it can elucidate the limitations of current ATDs under highly reclined conditions, guiding ATD development and providing theoretical guidance for future crash safety evaluations.

II. METHODS

Sled Environment

To explore the response of the occupant in the basic seat state, in this study, the sled collision used a rigid seat with zero-gravity characteristics. Rigid seats also have the advantages of easy processing, low cost, and good test repeatability. This seat features adjustable seat back, seat pan, and leg rest. These three rigid plates can be adjusted to any angle within the range of 25–70° with the vertical plane, 15–35° with the horizontal plane, and 5–79° with the vertical plane, respectively (Fig. 1). The angles of the seat back, seat pan, and leg rest can be adjusted together to achieve the desired seating position. The zero-gravity characteristic rigid seat is fixedly placed on the sled. The sled is not equipped with knee bolsters or foot supports. The restraint system in this study was provided by Autoliv and employed a seat-integrated three-point safety belt system. The seat back-integrated D-ring was installed on the upper right side of the seat back. The safety belt system was a conventional system with a shoulder-belt load limiter of approximately 4 kN. The belt pull-out length was set to 850mm. For the same purpose as using rigid seats, this study did not add additional restraint methods to the restraint system such as pretensioner and crash locking tongue in order to obtain base responses of the occupant. The results of this study can be used as a comparative analysis of the effects on occupants of seats with different stiffness and restraint systems in subsequent studies. The FE model of the safety belt's webbing was primarily established using 2D shell elements, with the shoulder and lap belt connections set as 1D elements at the slip rings, combined with a 2D slip-rings formulation to ensure smooth operation of the belt. Safety belt FE model matched that used in experimental sled tests. The shoulder belt was positioned to cross the middle of the clavicle, while the lap belt was routed low on the hips, touching the thighs, and kept snug and close to the bones as much as possible.

A pulse with a peak acceleration of 23g and a delta-v of 47 km/h was utilised (Fig. 1). The crash pulse was derived from 65 sedan and SUV collisions in MPDB test conditions conducted by China Automotive Engineering Research Institute Co., Ltd. from 2020 to 2023. To enhance the stability of pulse input during sled collision tests, the crash pulse from MPDB tests was averaged and further equivalent to a double trapezoidal wave based on the principle of momentum conservation. The sled model was verified by comparing the results of sled test and simulation.

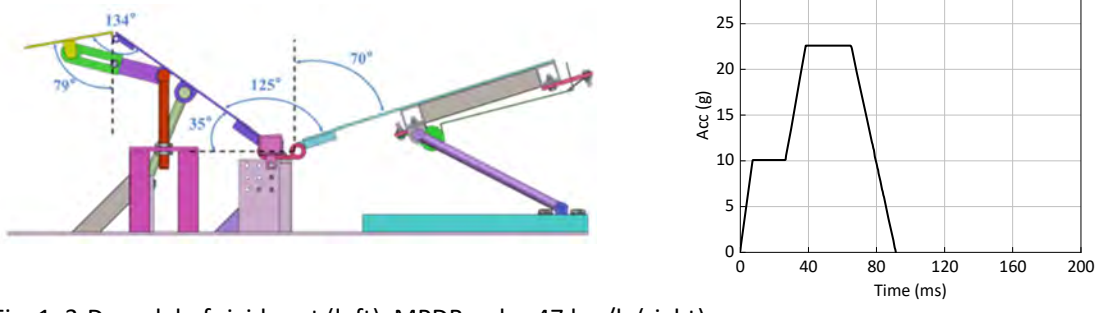

Fig. 1. 3-D model of rigid seat (left). MPDB pulse 47 km/h (right).

Simulation Matrix

Both the THOR-AV model and THUMS v6.1 were used. Four postures were designed for each model, resulting in a total of eight simulations. The simulation matrix is presented in Table I. The four postures were designed considering variations in the seat-back angle, seat pan angle, and leg rest status, with the seat-back angle ranging from 25° to 65°. When adjusting the seat angle, the seat-back angle was first adjusted, followed by the seat pan angle, and finally the leg rest angle. The seat-back angle refers to the angle between the seat-back and the vertical plane, while the seat pan and leg rest angles are recorded as the angles with respect to the horizontal plane after adjusting the seat. The posture with a seat-back angle of 25° and a seat cushion angle of 15° was designated as the upright standard posture.

TABLE I
SIMULATION MATRIX

Subject	Seating position	Seat back angle	Seat pan angle	Leg rest	Leg rest angle
THOR-AV	Standard	25°	15°	No	
THOR-AV	Reclined	45°	25°	No	
THOR-AV	Relaxed1	56°	15°	Yes	40°
THOR-AV	Relaxed2	65°	30°	Yes	30°
THUMS	Standard	25°	15°	No	
THUMS	Reclined	45°	25°	No	
THUMS	Relaxed1	56°	15°	Yes	40°
THUMS	Relaxed2	65°	30°	Yes	30°

ATD and HBM Positioning

The body structures of the two simulation objects naturally differ. THUMS features detailed human skeletal, visceral and muscular structures. THOR-AV notably improves the geometric shapes of the iliac wing and sacrum in the pelvic region to closely resemble human skeletal shapes, with the lumbar spine made of cylindrical rubber. The thoracic spine is composed of multiple mechanical components, connected by hinges at the midsection. The posture adjustments for THOR-AV and THUMS used a displacement-based spring-wire method. Initially, the posture of the THOR-AV model was adjusted based on posture data recorded from the THOR-AV 50M sled test. The THOR-AV 50M model has three angular versions: THOR-AV 25° model was used for posture adjustments at a seatback angle of 25°; THOR-AV 45° model for seatback angles of 45° and 56°; and THOR-AV 60° model for a seatback angle of 65°. Subsequently, to align the postures of THUMS and THOR-AV models, the H-point coordinates of both models were matched, and the pelvic angle of THUMS was globally adjusted to align the iliac wing angle with that of THOR-AV. Then, the angles of the lumbar spine, thoracic spine, head-neck, limbs, and feet of THUMS were sequentially adjusted. Due to THUMS being thinner compared to THOR-AV, particularly in the buttocks and thighs, after posture adjustment the Y-direction of THUMS remained unchanged, while the positions in the X and Z directions were further fine-tuned to ensure optimal contact between the body and the seat.

Data processing

THOR-AV model is equipped with the same sensor system as the dummy. THOR-AV is equipped with acceleration sensors at T1, T4 and T12, but the physical position cannot perfectly correspond to the T1, T4 and T12 vertebra of THUMS. By projecting the rigid block position of THOR-AV sensor onto THUMS, the marks of the motion trajectory output of THOR-AV and THUMS were determined (Fig. 2). The motion trajectories at T3, T9 and L2 of THUMS were extracted. The motion trajectory of H-point was extracted as the motion of the pelvis. There are two loadcells on the THOR-AV spine, which are located in the upper thoracic vertebra (T4) and the lower thoracic vertebra (T12). The T12 loadcell is above the flexible lumbar element. The lumbar and pelvis forces of THOR-AV were extracted from the corresponding loadcells with respect to local coordinate systems. The output settings for THUMS were based on the sensor outputs of THUMS v7. The lumbar spine forces and moments of THUMS were extracted from the sectional forces of the individual lumbar vertebral bodies with respect to a local coordinate system near the centre of gravity of each vertebra (Fig. 3). The local coordinate systems of lumbar vertebrae in THUMS were defined with the X-axis directed backward and the Z-axis directed upward, in contrast to the setting of THOR-AV. The lateral Y-axis was directed to both models' right. Pelvis iliac wings resultant forces of THUMS were measured using cross section force measurements with no local coordinate system. Taking the sacral upper plane center point of THUMS as the origin, the movement data of THUMS thoracolumbar vertebrae from T12 to L5 relative to this point at different time

points in four postures were processed. The output data from THOR-AV and THUMS were filtered with CFC600 for forces and moments according to SAE J211. Acceleration data for the head and pelvis were filtered with CFC1000.

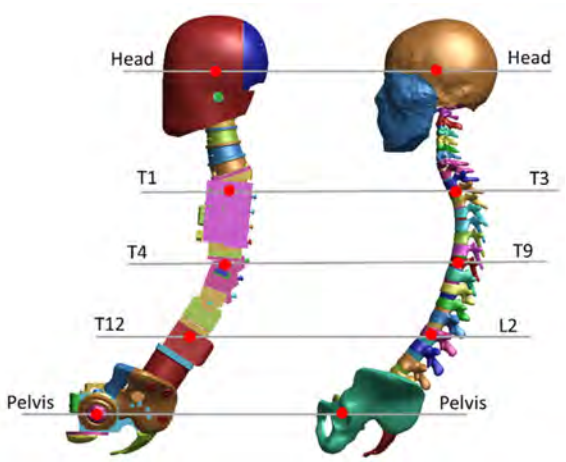

Fig. 2. Correspondence of trajectory tracking positions between THOR-AV and THUMS.

Fig. 3. Cross section definitions for lumbar spine vertebra L1 and pelvis iliac wing of THOR-AV (left) and THUMS (right). Intervertebral discs not shown for the lumbar spine of THUMS.

III. RESULTS

Sled FE model Validation

The sled environment was verified by THOR-AV under standard state (Fig. 4 and Fig. 5). Both the initial postures and the kinematics at the moment of maximum pelvic forward excursion of THOR-AV were consistent in the sled test and simulation (Fig. 4). Similar magnitude and shape of belt forces in test and simulation were measured. The head and pelvic X/Z accelerations also corresponded well in magnitude and shape (Fig. 5). Small differences in phase of these curves were observed. In the test, loose protective straps were wrapped around THOR-AV's lower legs and pelvis to protect it from serious damage and avoid reducing its repeatability. The straps can produce a little restraint effect during the movement of the THOR-AV, thus the dummy was restrained earlier. Take that into consideration, boundary forces and kinetic responses of THOR-AV generally compared well between the sled test and the simulation.

Fig. 4. Kinematics of THOR-AV in sled test and simulation at 0ms (left) and the moment of maximum pelvic forward excursion (right).

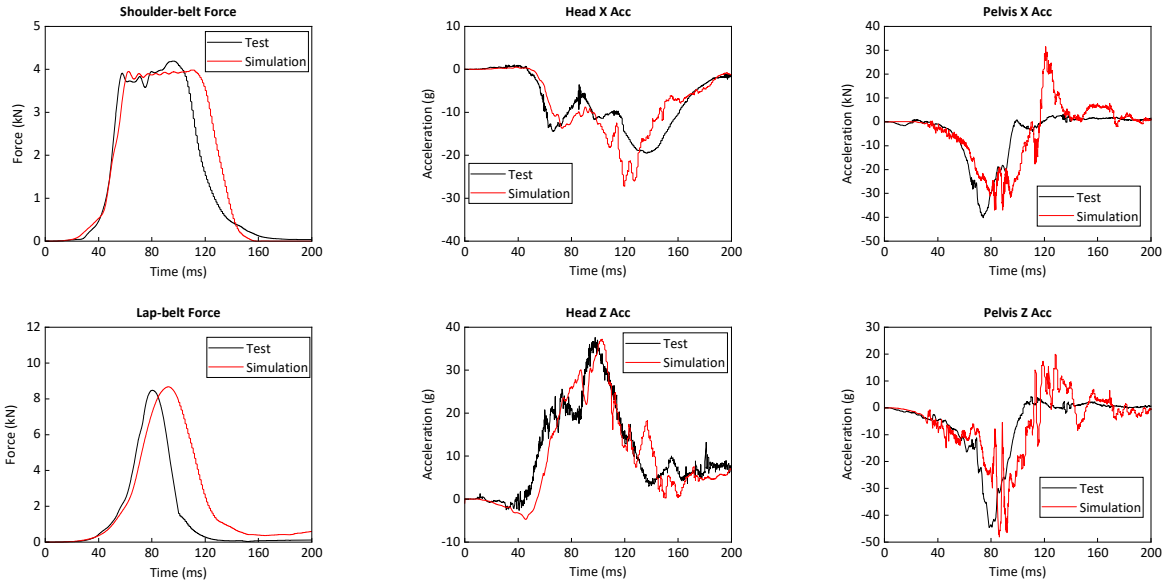

Fig. 5. Comparison between the kinetic responses of THOR-AV in sled test and simulation.

Whole Body Kinematics

The kinematics of THOR-AV and THUMS at 50 ms, 90 ms, and 130 ms in four seating positions are displayed in Fig. 6. Regardless of the seat angle, before the pelvis reached maximum forward displacement, the kinematics of both THOR-AV FE model and THUMS could match well. The torso further rotated forward towards the thighs and then rebounded. After the moment when the pelvis reached the forward displacement (approximately 90 ms), differences in the kinematics between THOR-AV and THUMS began to emerge. The torso of THUMS was softer compared to THOR-AV. For instance, at 130 ms in the standard posture and at 90 ms in Relaxed2 posture, it was clearly observed that the degree of torso bending in THUMS was more larger than in THOR-AV. Due to the design improvement of neck rubber in THOR-AV, there was high consistency in the motion rotation of the head and neck between THOR-AV and THUMS. As the posture changed with increases in the seat-back angle and the seat pan height, the forward rotation of the occupant's torso decreased, and the occupant's torso seemed to move more in accordance with the angles formed by the seat-back and seat pan.

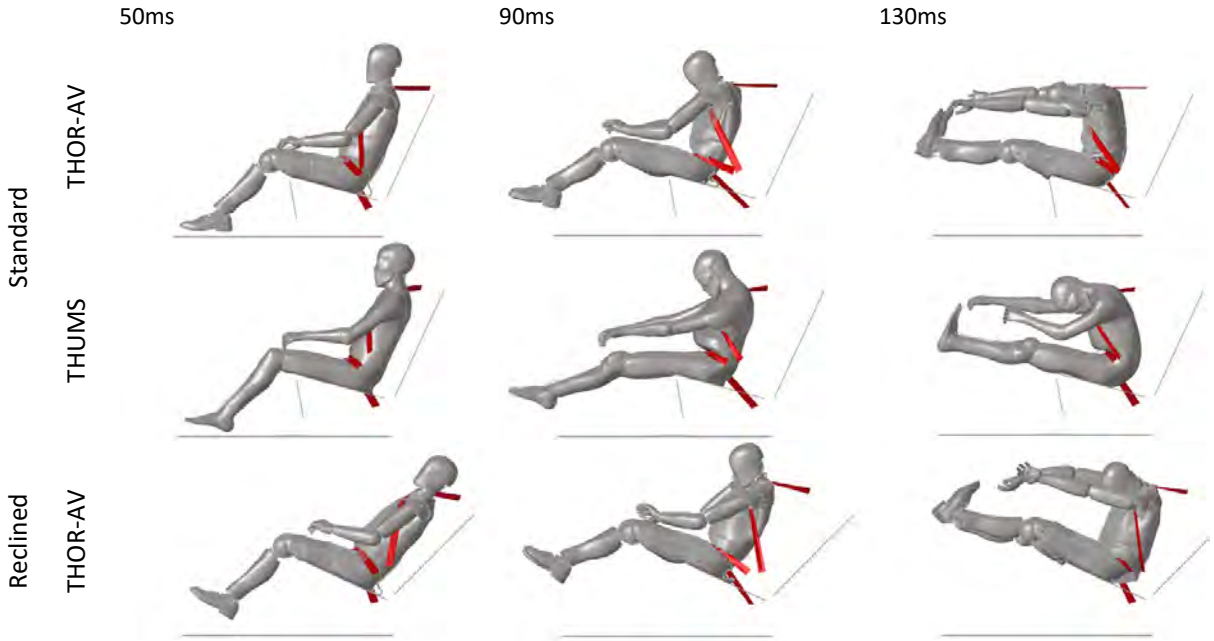

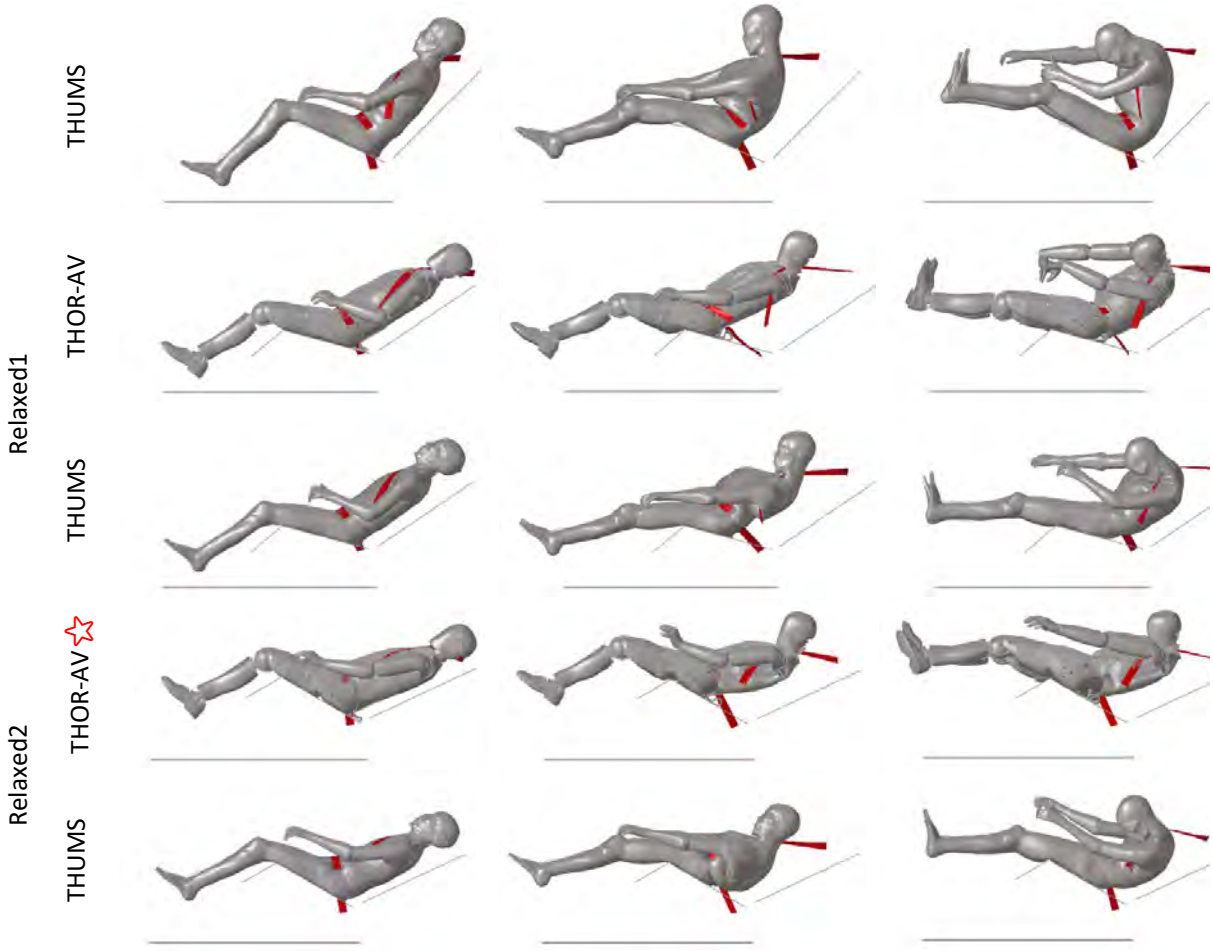

Fig. 6. Kinematics relative to the seat at 50, 90 and 130 ms.

Additionally, submarining was identified if the lower edge of the lap belt went over the anterior superior iliac spine (ASIS) on either side during the forward movement of the body by visual inspection in this study. THOR-AV submarined around 80ms (Fig. 6 and Fig. 7) in the Relaxed2 case. THUMS did not submarine in any posture. In the initial state of THOR-AV submarining case, the lap belt is closer to ASIS in the horizontal direction, and the angle between the lap belt and the horizontal plane is very small. The lap belt crossed the ASIS on the left side of the pelvis, but on the right side it was still in contact with the pelvis. In the post-submarining state, the lap belt on the left side directly loaded the abdomen.

Fig. 7. The motion of the lap belt and pelvis in the submarining case.

The motion trajectories of the head, T3, T9, L2, and the pelvis (H-point) of THUMS and THOR-AV in four different postures are illustrated in Fig. 8. The duration of the motion track was intercepted to 180 ms for visual clarity. The shapes of the motion trajectories of THOR-AV and THUMS were similar with the exception of the Relaxed2 posture. In the Relaxed2 state, all parts of the torso of THOR-AV with submarining moved upward, but T3, T9, and T12 of THUMS without submarining moved downward to varying degrees. The trends in pelvic motion corresponded well between the two models. The motion in the X direction of the head showed minimal differences, but in the upward Z direction the motion variation in THUMS was significantly more serious than in THOR-AV.

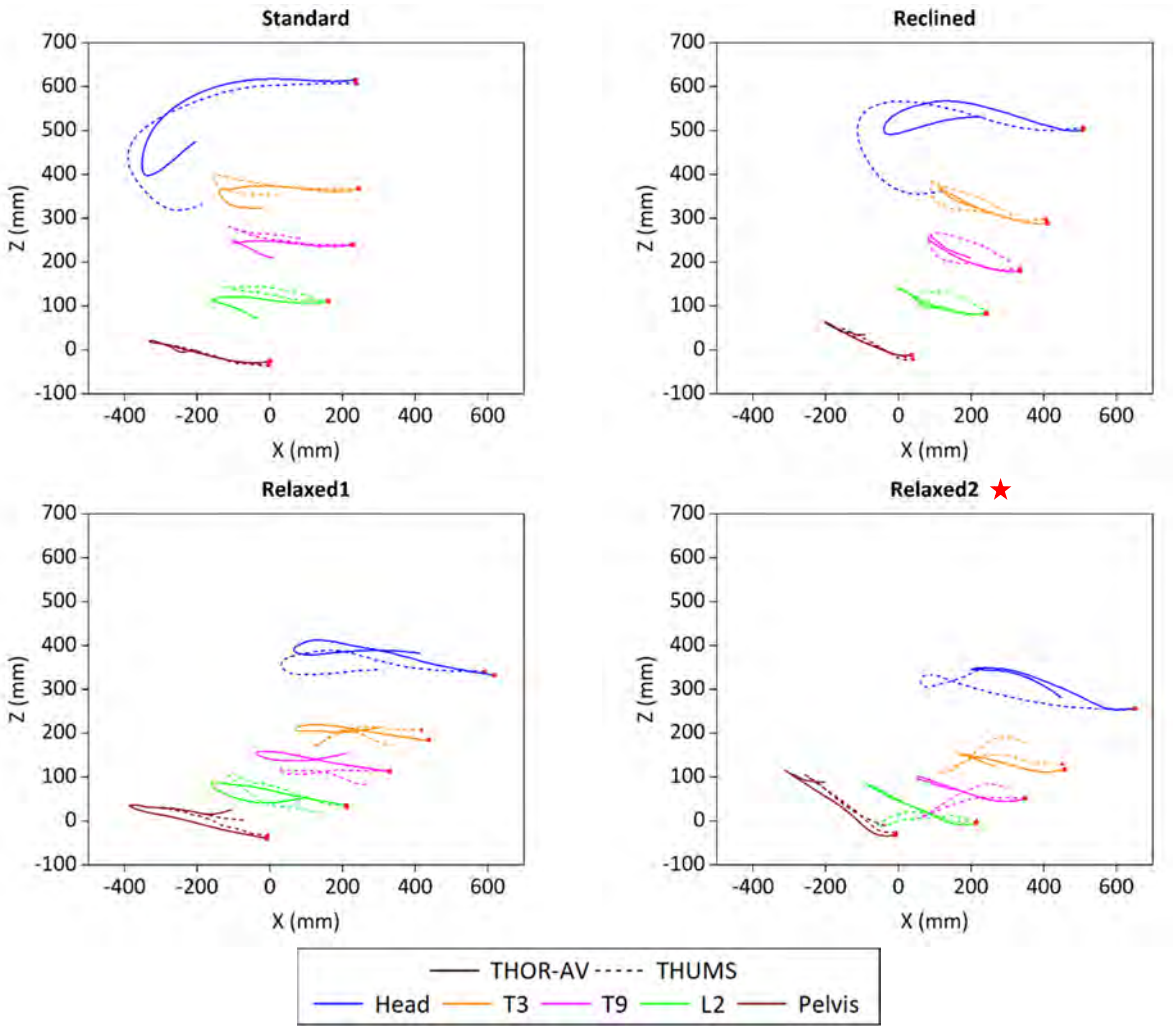

Fig. 8. Comparison of the movement trajectories of the head, T3, T9, L2, and the pelvis (H-point) of THUMS and THOR-AV in four sitting positions. The red signs indicate the initial position, the square is THOR-AV, and the triangle is THUMS.

Belt forces

In all four postures, the shoulder-belt forces reached the limit of 4 kN (Fig. 9). In the standard posture and the reclined posture, the shoulder belt forces of THOR-AV and THUMS were comparable. In the relaxed posture, the shoulder-belt force of THOR-AV exhibited a backward shift compared to THUMS, and the peak force occurred later. As the posture changed, there were significant variations in the peak values of the lap-belt force. The measured lap-belt force was set on the anchor side. The submarining of THOR-AV occurred on the buckle side rather than the anchor side in Reclined2 posture. There was no sudden drop in lap-belt force. The lap-belt force was greatest in THOR-AV in the Relaxed1 posture and smallest in THOR-AV in the Relaxed2 posture. THOR-AV had lower lap belt forces than THUMS in all postures except for the Relaxed1 posture. In the relationship between force and time, as the recline angle of the occupant increased, the loading of the seatbelt force was delayed. Both the shoulder-belt force and the lap-belt force started to rise earlier in THUMS compared to THOR-AV.

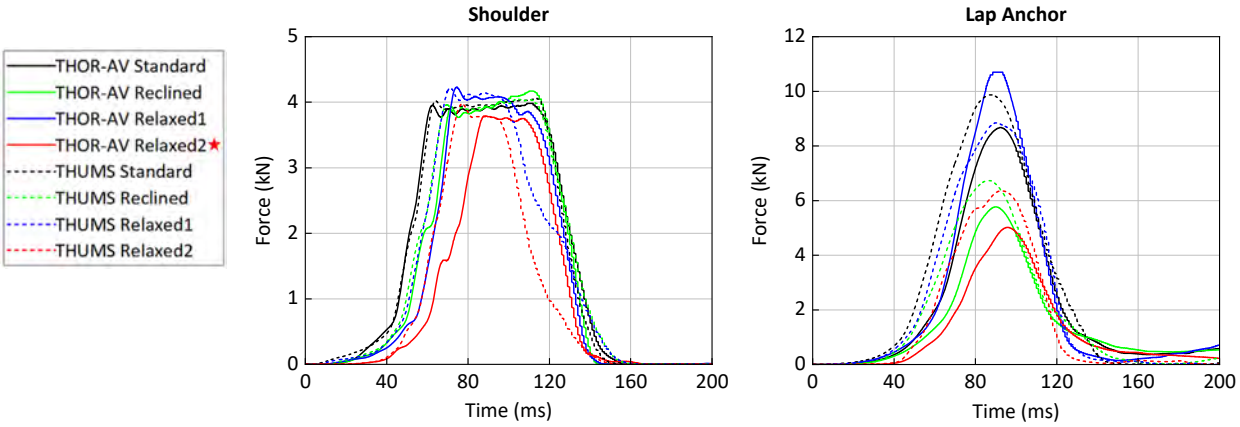

Fig. 9. Comparison of shoulder-belt force and lap-belt force of THUMS and THOR-AV belts in four sitting postures.

Pelvis

The maximum forward displacement of the occupant's pelvis (H-point) varied with the occupant type and posture (Fig. 10). In all four conditions, the pelvis forward displacement in THOR-AV was greater than that in THUMS. The maximum forward displacement of the pelvis was higher in the Relaxed1 posture compared to the standard posture, and in the Relaxed2 posture compared to the Reclined posture. In submarining case of THOR-AV in Relaxed2 posture, the pelvis X displacement could reach 300 mm. An increase in the seatback angle led to an increase in the pelvis forward displacement. Both lap-belt force and pelvis translation were maximal in the Relaxed1 posture. However, the pelvis motion of the occupant was less in the increased seat-pan angle posture compared to the standard seat-pan angle posture. An increase in the seat-pan angle effectively inhibited the forward displacement of the occupant's pelvis. The positive value in pelvis rotation indicated backward rotation of the pelvis (Fig. 10). In the four simulated postures, both occupants' pelvises initially rotated roughly backwards. And then the pelvic rotation of THOR-AV was maintained in the backward state for all four postures, including the submarining case. THUMS' pelvis rotated significantly forward during the rebound phase. The pelvis motion of THUMS was more flexible compared to THOR-AV.

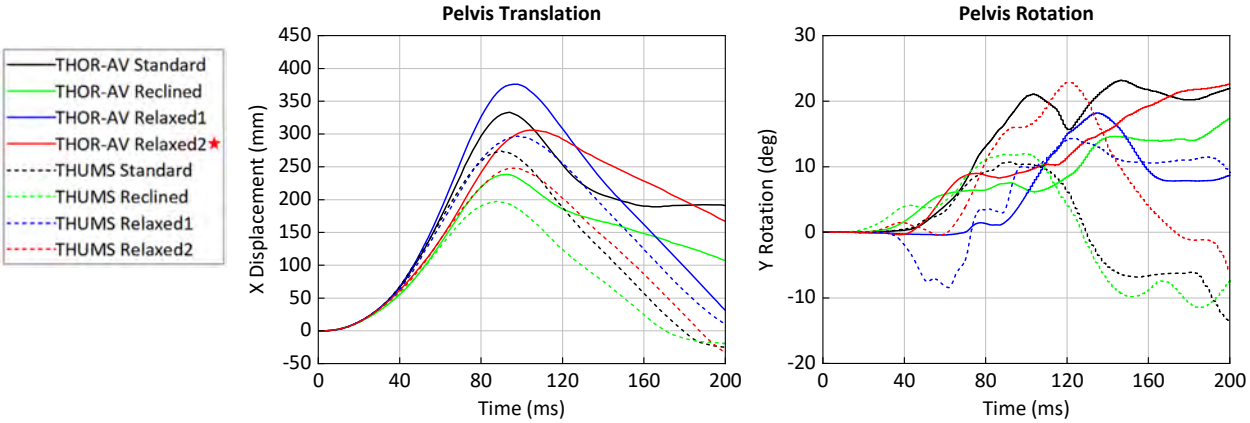

Fig. 10. Comparison of forward displacement and rotation of THUMS and THOR-AV pelvis in four sitting postures.

The resultant forces loading on the pelvis of THOR-AV and THUMS are shown in Fig. 11. In both THOR-AV and THUMS, the forces on the right iliac wing (anchor) were always greater than the forces on the left iliac wing (buckle). During motion, the right iliac wing of the occupant's pelvis has better engagement with the seatbelt. When comparing the iliac wing forces of THUMS/THOR-AV in Standard and Relaxed1 postures, it is observed that the iliac wing forces increase with an increase in the seatback angle. Notably, the iliac wing forces of THOR-AV were the lowest and the force on left iliac wing was much lower than that on the right iliac wing in the Relaxed2 posture. In this case, the pelvis and lap belt were in a more horizontal state, the lap belt's contact with the pelvis was light throughout the motion. In addition, with the submarining on left side of pelvis at 80ms, the left iliac wing force began to decrease, resulting in the left iliac wing force less than 1kN.

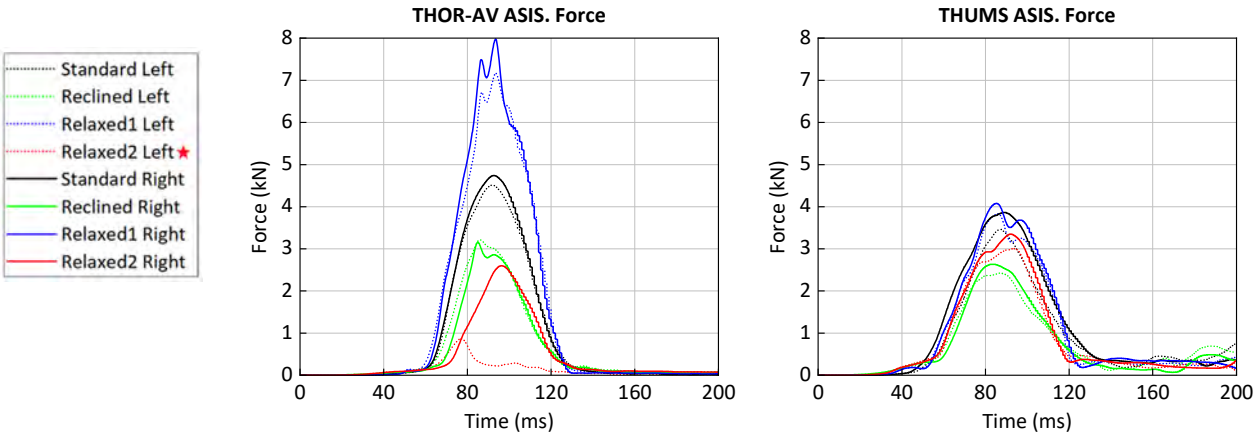

Fig. 11. Comparison of left and right A.S.I.S resultant force between THOR-AV and THUMS.

Thoracolumbar Spine

The force and moment directions output by THOR-AV and THUMS were processed to be unified, negative values of force for T12 represent axial compression, and negative values of moment represent flexion (Fig. 12). In the same posture, the T12 compression force and flexion moment of THOR-AV were both higher than those of THUMS. In the Relaxed1 posture, the T12 compression force for the lumbar vertebrae of THOR-AV and THUMS were the highest, at 10 kN and 5 kN, respectively. In the Standard posture, the T12 forces for both models were the lowest, at 5 kN and 3.5 kN, respectively. In submarining case of THOR-AV in Relaxed2 posture, the T12 peak compression force was 6kN, and the flexion was lowest among four postures. As the posture changed, the peak compression force of T12 in THOR-AV varied, and the moments at the same time when compression force peaked were different. The flexion moment of T12 in THOR-AV was far higher than that of THUMS, with the peak moment occurring about 50 ms later. The variations in peak compression force and flexion moment of THUMS T12 in four different postures were relatively low, with the peak force moments more concentrated. The loading in THUMS was more stable than THOR-AV in this study.

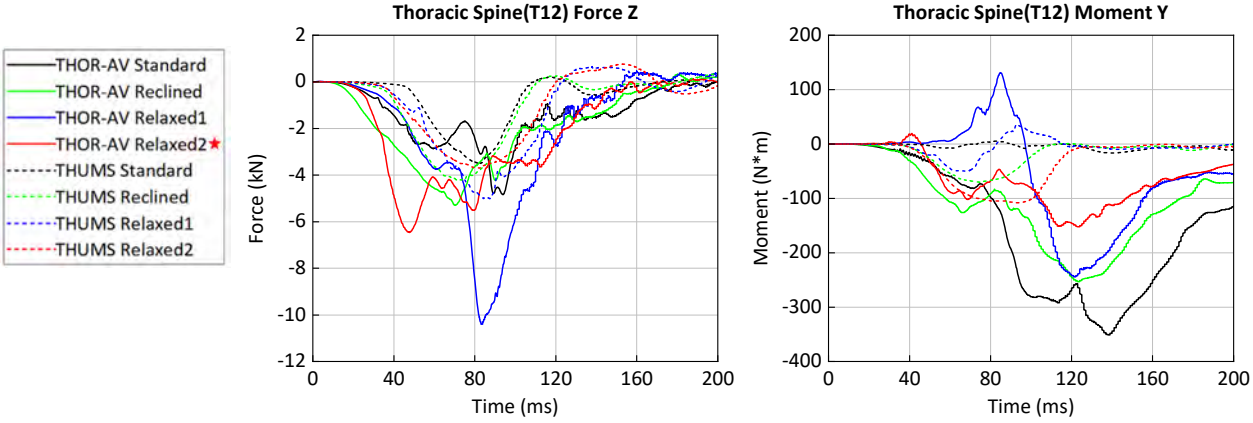

Fig. 12. Axial compression force and flexion moment of THOR-AV and THUMS thoracic vertebrae T12.

The changes in lumbar vertebrae movement of THUMS are shown in Fig.13. In the Standard posture, the THUMS lumbar vertebrae moved forward, with a noticeable flexion at L3. In the Relaxed1 posture, the THUMS lumbar vertebrae first exhibited a backward extension during the forward motion, then rebounded past the initial spinal position. In the Reclined posture and the Relaxed2 posture with increased angles of seat-back and seat-pan, the THUMS lumbar vertebrae first moved backward, then returned at 90 ms and rotated forward. In the Reclined posture, almost all lumbar vertebrae exhibited flexion. In the Relaxed2 posture, the lumbar vertebrae pivoted at L3, with the T12-L3 flexing forward and the L4-L5 extending backward.

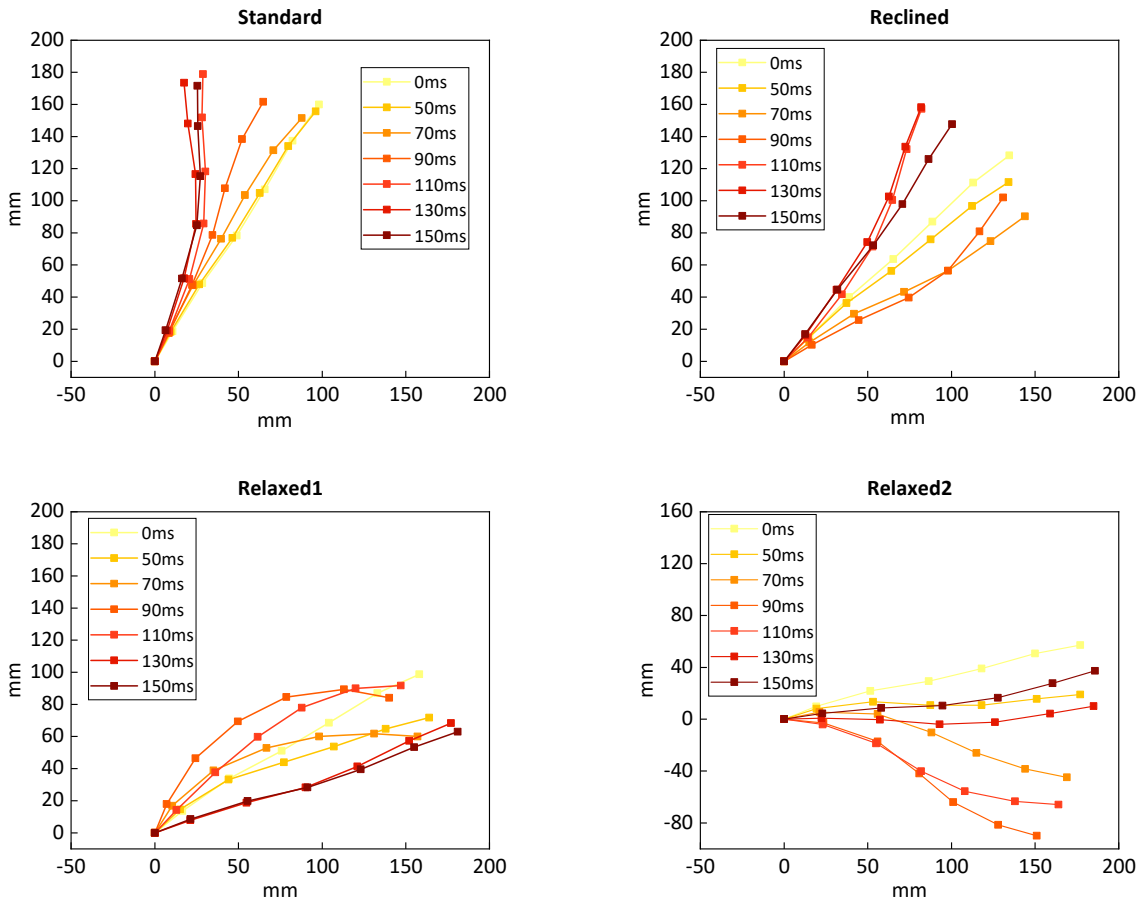

Fig. 13. Movement changes of T12-L5 vertebrae of THUMS in four postures.

The maximum load of human lumbar spine is different in varied postures, and the load of different vertebra in the same posture is also different (Fig. 14). The maximum compression force changing trends for T12 to L5 in the Standard and Reclined1 postures were similar, with the maximum compression force decreasing first and then increasing. In the Relaxed1 posture, the T12 bore a compression force of 5 kN, the highest among all THUMS simulations. In the Reclined posture and the Relaxed2 posture, the magnitudes of force loaded on different vertebra were similar, with the maximum compression force on L1. The variations in compression force borne by different lumbar vertebrae in THUMS postures without an increased seat-pan angle differed significantly from those in postures with an increased seat-pan angle. In particular, extension moments were observed in some lumbar vertebra in the Relaxed1 and Relaxed2 postures. In the Relaxed1 posture, the L3 vertebra bore an extension moment. In the Relaxed2 posture, the moment borne by the lumbar vertebrae from T12 to L5 gradually transitions from flexion moment to extension moment. In the Relaxed2 posture, T12 bore the highest flexion moment at 110 N*m, followed by L2 in the Reclined posture and L5 in the Relaxed1 posture, both bearing a flexion moment close to 100 N*m. During simulations, the lumbar vertebrae were subjected to a composite load. With the change of the initial posture, the load on the lumbar vertebrae could transition from compression-flexion to compression-extension.

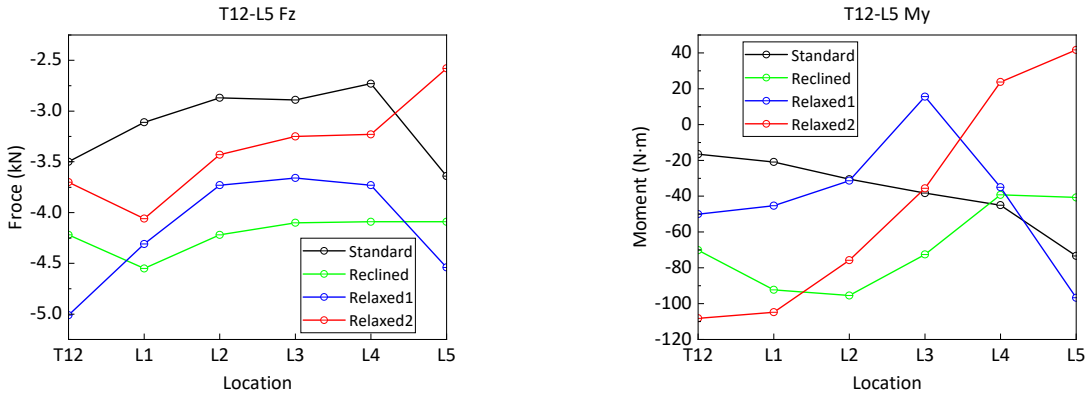

Fig. 14. The maximum axial force and moment of T12-L5 vertebrae from THUMS.

IV. DISCUSSION

The THOR-AV dummy is specially developed for evaluating occupant injuries in autonomous vehicle tests. THUMS, a human FE model developed by Toyota, allows for a more detailed analysis of injuries during collisions. As two tools used for assessing occupant impact injuries, THOR-AV model and THUMS demonstrate comparability in kinematics and dynamic responses. Utilising rigid seats for sled simulations, the kinematics of the two models were similar during the collision process, especially before the pelvis reached its maximum forward displacement. After the pelvis reached the maximum forward displacement, the torso would rotate further forward, reaching the maximum rotation before rebounding. During this period, the two models gradually showed some differences in motion, primarily manifested in THUMS having a higher degree of torso bending than THOR-AV, as observed in both Standard and Relaxed2 postures. Despite variations in sensor positions of body parts between THOR-AV mode and THUMS, the captured data on motion displacement and forces at corresponding body parts still effectively reflected the similarities and differences in the motion responses of both models.

Compared to THOR-AV, THUMS exhibited less forward displacement of the pelvis, but the trend of maximum forward displacement of the pelvis changed similarly as the posture varied between the two models. This may be attributed to the design of the pelvis, spine and muscle structures, and the interaction between the models and the seat. THUMS model incorporates realistic muscle tissues that envelop the skeleton. During motion, the thigh and hip muscles of THUMS came into contact with the rigid seat pan, providing a cushioning effect against collision impacts. The motion trajectories of the pelvis (H-point) of both models aligned well. THOR-AV features a realistic coccyx and iliac wing shape in the pelvis [16], with a size that is also comparable to that of THUMS. When adjusting posture, the pelvis angle of both models was the first to be aligned, with the H-point coordinates being adjusted first before sequentially rotating the pelvis of THUMS to correspond the iliac wing of both models. As the posture transitions from Standard to Reclined postures, the pelvis displacement of both models followed a similar pattern. For example, as the seatback reclined angle increased, the forward displacement of the pelvis also increased. Adjusting the seat-pan angle can effectively reduce the forward displacement of the pelvis, a pattern also observed in [18].

Submarining occurs when the belt crosses either side of the iliac during forward motion. According to this definition, THOR-AV submarined on the left side of the body in Relaxed2 posture in this study. The submarining is accompanied by a decrease in iliac wing force on the corresponding side, which is consistent with the findings in [19-20]. The occurrence of submarining is related to the initial lap belt-pelvis engagement and the rotation of the pelvis during the motion. As the reclined angle changes, the shape of the seat belt becomes more horizontal. Also, differences in the external surface contour of THOR-AV and THUMS resulted in a somewhat different geometry of the lap belt. In the submarining case of THOR-AV (seatback 65°, seat pan 30°), the initial distance between the lap belt and ASIS was closer in the X direction and farther in the Z direction, and the pelvis continued to rotate backward during the motion. It is worth mentioning that lap belt crossed the left ASIS during the rebound stage (about 130ms) of THOR-AV and THUMS in Relaxed1 posture and THUMS in relaxed2 posture. But due to the seat belt force have been unloaded many, so the results of the pelvis-lap belt motion in these cases were not discussed.

From a timing perspective, the moments of maximum forward displacement of the pelvis, peak lap-belt force, and peak iliac wing force were relatively close. The lap-belt force was greater than the iliac wing force, and the iliac wing force at the anchor point was higher, consistent with findings in [15] . Under the Relaxed posture with a seatback angle of 56° and a seat-pan angle of 15°, the model showed the highest load on the pelvis. Models with increased seat-pan angles always had lower pelvic forces compared to models with standard seat-pan angle. Increasing the seat-pan angle not only reduces pelvis forward displacement but also decreases pelvis loading. Apart from the Relaxed2 posture, THUMS generally showed lower iliac wing forces compared to THOR-AV, but higher lap-belt forces, possibly related to the connection and interaction between the model's pelvis and surrounding muscles. When increasing both the seatback angle and seat-pan angle

significantly, the occupant response in this posture may have some unique characteristics, and it cannot be guaranteed that the changes in force response of the two models will be the same. Further research is needed to quantitatively analyse the responses of the two models under special posture designs.

The rotation of the pelvis and the flexion-extension of the lumbar spine play a significant role in lumbar spine injuries[9,21]. The rotation of the pelvis in the two models was not consistent. THOR-AV tends to exhibit sustained posterior pelvic rotation, while THUMS gradually returns to anterior rotation after reaching a certain peak of posterior rotation. This difference may be attributed to the stiffer buttocks soft tissues of THOR-AV, which are less likely to compress during interaction with the seat belt, resulting in reduced coupling between the pelvis and the seat pan, leading to sustained posterior pelvis rotation. In this study, the measured flexion moments at T12 in the THOR-AV dummy model were generally higher than those in THUMS, and they were difficult to correspond in time. The difference in pelvic rotation between the two models can partially explain this phenomenon. The occurrence may also be related to the lumbar spine design of THOR-AV. The lumbar spine of THOR-AV is designed as a single cylindrical rubber block. The lumbar vertebrae of THUMS are arranged sequentially with deformable and flexible intervertebral discs between them, providing better overall compliance of the spine, resulting in more stable force distribution from the seat to the pelvis and spine. This also explains why the force and moment outputs at T12 of THUMS are smoother compared to THOR-AV. The differences in lumbar spine stiffness and pelvic rotation will also lead to different vertical behaviors measured along the chain from the L3 to the head in the two models. THUMS showed relatively good agreement with THOR-AV in X direction trajectory, however the discrepancies in Z directions were larger. This phenomenon is similar to the findings in [11], which compared the responses of HBMs and PMHS. The lumbar spine model of THUMS is too compliant under large flexion load. The data suggest that the difference between THOR-AV and THUMS is largely due to differences in lumbar spine response. It is also due to the different load path offloading the lumbar spine in THUMS and THOR-AV. THOR-AV requires a spine that is stiff enough to bear the load and support the movement of the entire torso. However, THUMS have some muscle and fat in addition to the spine to carry the load, and its load path is more complex. In the postures with leg rest support, as the body starts to move, the legs move forward and detach from the leg rest support tray, the kinematic impact of the leg support on the occupant is not considered in this study for now.

As posture changes, the trend of compression force output at T12 in both THOR-AV and THUMS was consistent, with the highest values observed in the Relaxed1 posture, followed by the Reclined and Relaxed2 postures, and the lowest in the Standard posture. Increasing the seatback angle alone often results in higher lumbar spine compression force (Fz), but this can be mitigated by raising the seat-pan angle. It is important to note that the peak compression force at the T12 lumbar spine observed in the simulation generally occurs at a different time from the peak moment, indicating that spinal loading is the result of various forms of loads together. In actual accidents, occupants may experience different types of spinal injury due to varying load forms. Recent research in [22-23] conducted compressive bending tests on cadaveric lumbar spine segments and proposed a structural formula L_{fx} with components Fz and My as indicators to evaluate the risk of lumbar spine injuries. The studies found that the proportion of force and moment in the lumbar spine L_{fx} index of the GHBMC differs from that of PMHS lumbar spine. Particularly, when the seatback angle is sufficiently large, the lumbar spine may experience extension moments. In this study, extension phenomena were observed in the L3 vertebrae in the Relaxed1 posture with a seatback angle of 56°, and in the L4 and L5 vertebrae in the Relaxed2 posture with a seatback angle of 65°. Similar extension phenomena were also noted in a PMHS test tilted at 58° in [24]. The T12 to L5 vertebrae are likely to suffer the most severe load and the load distribution may vary among different vertebrae in specific sitting postures. Future research needs to delve deeper into the load forms and resulting injuries of highly reclined human lumbar spine injuries. The THOR-AV dummy for large recline postures also requires further exploration in terms of lumbar spine injury metrics and limits.

V. CONCLUSION

This study primarily investigated the similarities and differences in collision responses between the dummy model (THOR-AV) and the HBM (THUMS) under rigid seat with zero gravity characteristics, and explored the variations in kinematics loads of the two models with changes in seat angles, focusing on the pelvic-lumbar spine dynamics of both models. Through simulations in four different postures, it was found that the displacement response of the pelvis in THOR-AV and THUMS is relatively consistent, but there were differences in pelvic rotation. In this study, the pelvis of THOR-AV exhibited more posterior rotation, while the pelvis of THUMS underwent initial posterior rotation followed by forward rotation. Due to the difference of the lumbar spine response, the Z-direction displacement along the lumbar spine motion chain in THUMS was larger in THOR-AV. The changes in compression force at T12 measured with posture variations in THOR-AV and THUMS are similar, suggesting a potential mapping relationship at T12, but the two models exhibit inconsistent and significant differences in the moments at T12. The vertebral body load forms from T12 to L5 differ across different postures. Further research is needed to explore the mechanisms of lumbar spine injuries in different collision test subjects.

VI. ACKNOWLEDGEMENTS

The authors acknowledge Humanetics for providing the FE model of THOR-AV dummy. We are also very grateful to

Autoliv Research, for providing the FE model of the restraint system used in this study.

VII. REFERENCES

[1] Filatov, A., Scanlon, J. M., Bruno, A., Danthurthi, S. S. K., Fisher, J. (2019) Effects of innovation in automated vehicles on occupant compartment designs, evaluation, and safety: a review of public marketing, literature, and standards.

[2] Jorlöv, S., Bohman, K., Larsson, A. (2017) Seating positions and activities in highly automated cars–a qualitative study of future automated driving scenarios. *Proceedings of the IRCOBI Conference,* 2017, Antwerp, Belgium.

[3] Östling, M. and Larsson, A. (2019) Occupant activities and sitting positions in automated vehicles in China and Sweden. *Proceedings of 26th International Technical Conference on the Enhanced Safety of Vehicles (ESV),* 2019, Eindhoven, Netherlands.

[4] Liers, H. and Unger, T. (2019) Prediction of the expected accident scenario of future Level 2 and Level 3 cars on German motorways. *Proceedings of the IRCOBI Conference*, 2019, Florence, Italy.

[5] Saadé, J., Chajmowicz, H., Cuny, S. (2019) Prospective evaluation of the effectiveness of autonomous emergency braking systems in increasing pedestrian road safety in France. *Proceedings of the IRCOBI Conference*, 2019, Florence, Italy.

[6] McMurry, T. L., Poplin, G. S., Shaw, G., Panzer, M. B. (2018) Crash safety concerns for out-of-position occupant postures: A look toward safety in highly automated vehicles. *Traffic Injury Prevention*, **19**(6): pp. 582–587.

[7] NHTSA Test Report, https://www.nhtsa.gov/research-data/research-testing-databases#/biomechanics. Test numbers 12795, 12796, 13109, 13110, 13119, 13124.

[8] Richardson, R., Donlon, J-P., Jayathirtha, M. Forman, J., Shaw,G., Gepner, B., Kerrigan, J., Östling, M., Mroz, K., Pipkorn, B. (2020) Kinematic and injury response of reclined PMHS in frontal impacts. *Stapp car crash journal*, **64**: pp. 83-153.

[9] Richardson, R., Jayathirtha, M., Chastain, K., Donlon, J-P., Forman, J., Gepner, B., Östling, M., Mroz, K., Shaw, G., Pipkorn, B., Kerrigan, J. (2020) Thoracolumbar spine kinematics and injuries in frontal impacts with reclined occupants. *Traffic injury prevention*, **21**(sup1): S66-S71.

[10] Shin, J., Donlon, J. P., Richardson, R., Espelien, C., Sochor, S., Gallaher, M., Luong, V., Gepner B. Forman, J., Östling, M., Kerrigan, J. (2023) Comparison of thoracolumbar spine kinematics and injuries in reclined frontal impact sled tests between mid-size adult female and male PMHS. *Accident Analysis and Prevention*, **193**.

[11] Gepner, B., Perez-Rapela, D., Forman, J., Ostling, M., Pipkorn, B., Kerrigan, J. (2022) Evaluation of GHBMC, THUMS and SAFER Human Body Models in Frontal Impacts in Reclined Postures. *Proceedings of the IRCOBI Conference*, 2022, Porto, Portugal.

[12] Mroz, K., Östling, M., Richardson, R., Kerrigan, J., Forman, J., Gepner, B., Lubbe, N., Pipkorn, B. (2020). Effect of seat and seat belt characteristics on the lumbar spine and pelvis loading of the SAFER human body model in reclined postures. *Proceedings of Proceedings of the IRCOBI Conference*, 2020, Munich, Germany.

[13] Rawska, K., Gepner, B., and Kerrigan, J. (2021) Effect of various restraint configurations on submarining occurrence across varied seat configurations in autonomous driving system environment. *Traffic injury prevention*, **22**(sup1): p. S128-S133.

[14] Mishra, E., Lubbe, N. (2024) Assessing injury risks of reclined occupants in a frontal crash preceded by braking with varied seatbelt designs using the SAFER Human Body Model. *Traffic injury prevention*, **25**: p. 445-453.

[15] Shin, J., Donlon, J. P., Richardson, R., Gepner, B., Forman, J., Östling, M., Kerrigan, J. (2022) Biofidelity Evaluation of the Hybrid-III 50th Male and THOR-50M in Reclined Frontal Impact Sled Tests. *Proceedings of the IRCOBI Conference*, 2022, Porto, Portugal.

[16] Wang, Z. J., Richard, O., Lebarbé, M., Uriot, J., Kabadayi, E., Kleessen, C. (2022) Biomechanical Responses of THOR-AV in a Semi-Rigid Seat that Mimics the Front and Rear Seat of a Midsize Car. *Proceedings of the IRCOBI Conference*, 2022, Porto, Portugal.

[17] Wang, Z. J., Zaseck, L. W., Reed, M. P. (2022) THOR-AV 50th Percentile Male Biofidelity Evaluation in 25 and 45 Seatback Angle Test Conditions with a Semi-Rigid Seat. *Proceedings of IRCOBI Conference*, 2022, Porto, Portugal.

[18] Rawska, K., Gepner, B., et al. (2019) Submarining sensitivity across varied anthropometry in an autonomous driving system environment. *Traffic Injury Prevention*, 20(sup2): pp. S123–S127.

[19] Gepner, B., Draper, D., et al. (2019) Comparison of human body models in frontal crashes with reclined seatback. *Proceedings of the IRCOBI Conference*, 2018, Florence, Italy.

[20] Gepner, B., Toczyski, J., Rawska, K., Moreau, D., Kerrigan, J. (2020) Sensitivity of human body model response relative to the lumbar spine and pelvic tissue formulation. *Proceedings of the IRCOBI Conference*, 2020, Munich, Germany.

[21] Richardson, R., Jayathirtha, M., et al. (2020) Pelvis kinematics and injuries of reclined occupants in frontal impacts. *Proceedings of the IRCOBI Conference*, 2020, Munich, Germany.

[22] Tushak, S. K., Donlon, J. P., et al. (2022) Failure tolerance of the human lumbar spine in dynamic combined compression and flexion loading. *Journal of Biomechanics*, 135: p. 111051.

[23] Tushak, S. K., Gepner, B. D., et al. (2023) Human lumbar spine injury risk in dynamic combined compression and flexion loading. *Annals of Biomedical Engineering*, 51(6): pp. 1216–1225.

[24] Richard, O., Uriot, J. (2022) Investigation of potential injury patterns and occupant kinematics in frontal impact with PMHS in reclined postures. *Stapp car crash journal*, 66: pp. 1-30.